

Synthesis of tin nanoparticles through modified polyol process and effects of centrifuging and drying on nanoparticles

Sang-Soo CHEE, Jong-Hyun LEE

Department of Materials Science and Engineering, Seoul National University of Science and Technology,
Seoul 139-743, Korea

Received 21 May 2012; accepted 5 November 2012

Abstract: Sn nanoparticles with average diameter of 13.1 nm were synthesized by modified polyol process, and their melting point was observed to be about 40 °C less than that of bulk Sn. Even though Sn nanoparticles are solid and covered with thin PVP capping and oxide layer, Sn nanoparticles in solution agglomerate upon centrifugation, resulting in a melting point increase. Owing to stickiness of the PVP capping layer, extensive aggregation between Sn nanoparticles was observed after drying. However, the aggregation behavior did not further influence the melting point, because actual agglomeration did not occur in the aggregates.

Key words: tin nanoparticle; melting point; centrifugation; agglomeration; aggregation

1 Introduction

With the growing interest in nano-materials, extensive studies have been conducted on pure metal nanoparticles such as copper, silver, gold, palladium, and platinum [1]. In particular, methods for fabrication of tin nanoparticles have been frequently proposed in recent years [2–10]. Tin is predominantly considered as a solder material, which has long been used as a representative interconnection material in microelectronic applications. Thus, the application of tin nanoparticles in the form of paste or ink materials is preferred for the interconnection in microelectronic applications. As the demand for fine-pitch printing and interconnection of components is continuously increasing, tin nanoparticles can be considered as a practically applicable material in the near future. Furthermore, considerable research has been focused on the decrease in the melting point of these nanoparticles with the decrease in their size and the use of this phenomenon for developing novel interconnection techniques to replace conventional soldering. Tin ink is also being considered a novel topic of research mainly owing to its low raw material cost [10]. In addition to the already low melting point of tin ink, it is expected that the decrease in the melting point on a nanoscale results in the formation of sufficiently sintered structures by the

nanoparticles in the ink even at a low sintering temperature or after a short sintering duration.

Although diverse fabrication processes of tin nanoparticles, including synthesis and break-up methods, have been reported [2–10], there have been few studies on the post-process effects on the nanoparticles. Nevertheless, tin nanoparticles synthesized through a wet reduction method may be subjected to post-process treatments such as centrifuging and drying.

In this work, the effect of centrifuging and drying on tin nanoparticles in a solution containing nanoparticles was investigated. The morphology of tin nanoparticles was analyzed before and after centrifuging and drying. To quantitatively evaluate the agglomeration and aggregation of Sn nanoparticles, differential scanning calorimetry (DSC) was conducted before and after centrifuging and drying the solution.

2 Experimental

Tin nanoparticles were synthesized through a modified polyol method involving the compulsory addition of a reducing agent at room temperature. Tin(II) 2-ethylhexanoate ($C_{16}H_{30}O_4Sn$, about 95%, Sigma-Aldrich Chemical Co.) and sodium borohydride ($NaBH_4$, 99.99%, Aldrich Chemical Co.) were used as a precursor agent and a reducing agent, respectively. The synthesis

also involved diethylene glycol (DEG, 99%, Sigma-Aldrich Chemical Co.) and polyvinylpyrrolidone (PVP, $M_w=1300000$, Aldrich Chemical Co.) as a reaction medium and capping material, respectively.

In a typical synthesis procedure, 1 g PVP and 2 g sodium borohydride were dissolved completely in 100 mL DEG for 1 h. Tin(II) 2-ethylhexanoate was injected into the DEG solution using a dispenser with constant stirring at room temperature. The injection rate was 4.5 mL/min. After the immediate initiation of the reduction reaction, the solution was continuously stirred using a magnetic stirrer for 1 h.

DEG cannot be dried easily, owing to its low volatility at room temperature. Hence, it was exchanged with methanol after each centrifugation; the solution was centrifuged four times. To verify the effect of centrifugation rate during centrifugation and solvent exchange on Sn nanoparticles, the solution containing synthesized nanoparticles was centrifuged for 30 min for each run at the centrifugation rate varying from 6000 to 12000 r/min. After centrifugation, the size and morphology of the tin nanoparticles in solution were observed using a transmission electron microscope (TEM) (Tecnai G² F30ST, FEI Company). Samples for the observation were prepared by dropping a solution on copper grids coated with carbon.

The resultant methanol solution containing Sn nanoparticles was dried in a vacuum chamber at room temperature. The size and morphology of the dried Sn nanoparticles were also observed, using a field emission scanning electron microscope (FE-SEM) (S-4800, Hitachi Ltd.).

To measure the variations in melting points during agglomeration or aggregation of the Sn nanoparticles, thermal analysis was conducted using a differential scanning calorimeter (Q20, TA Instruments). In the experiment on the solution containing Sn nanoparticles, no lid was used to cover the pan containing the sample during measurement in order to allow free evaporation of solvent. The pan was heated from 30 °C to 250 °C at a rate of 10 °C/min. To prevent oxidation during heating, nitrogen gas was blown over the pan at a rate of 50 mL/min.

3 Results and discussion

The size and morphology of as-synthesized Sn nanoparticles, synthesized via the modified polyol process, are shown in Fig. 1. The nanoparticles were spherical shapes with diameters of 6–20 nm (average diameter: 13.1 nm). In the high-magnification image under TEM (Fig. 1(b)), Sn crystallites are clearly observed in core regions whereas amorphous structures are observed to form in thin outer regions. In a similar

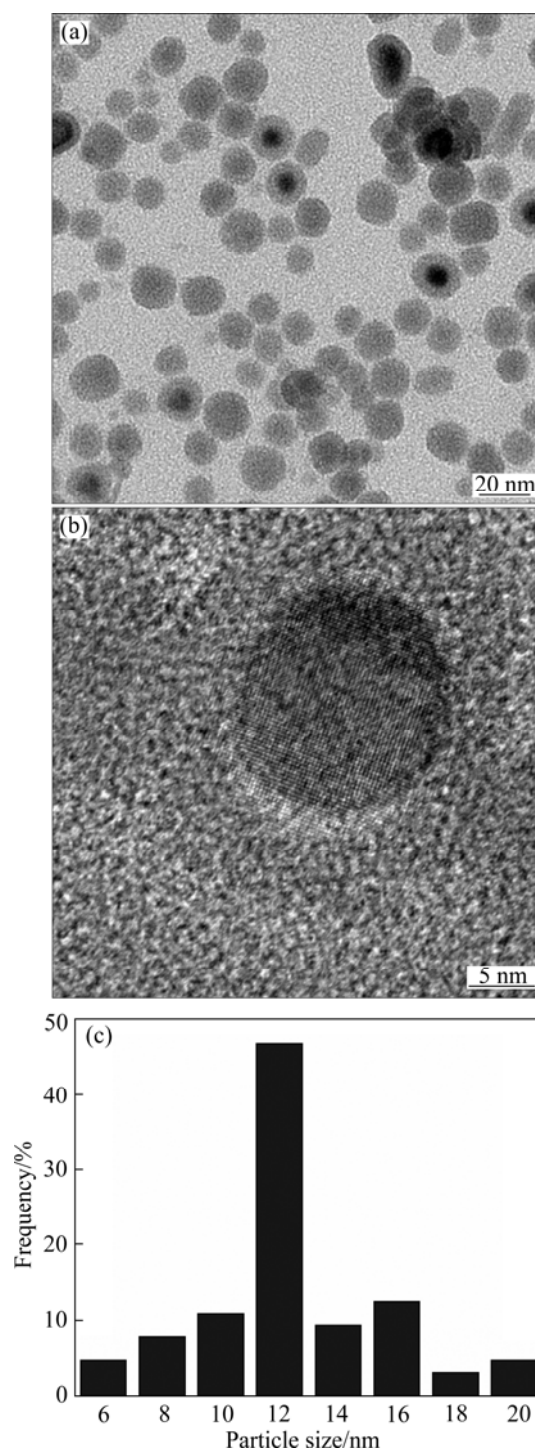
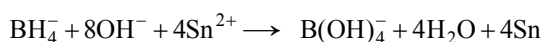


Fig. 1 TEM images of Sn nanoparticles as-synthesized by modified polyol process at (a) low magnification and (b) high magnification, and (c) Size distribution of nanoparticles

study [9], it was reported that the surface oxide layer of Sn nanoparticles synthesized through a reduction reaction in the solvent was amorphous. The reduction of Sn ions supplied from the precursor could be represented by the following reaction:



The TEM morphology of Sn nanoparticles at varying rates of centrifugation is shown in Fig. 2; this morphology is dependent on the rate of centrifugation that is conducted to exchange DEG with methanol. Centrifugation at 6000 r/min induced pronounced agglomeration of Sn nanoparticles, as shown in Fig. 2(a). As the centrifugation rate was increased from 6000 to 12000 r/min, the extent of agglomeration was observed to be slightly greater. An increase in the centrifugal force resulted in an enhanced agglomeration that promoted

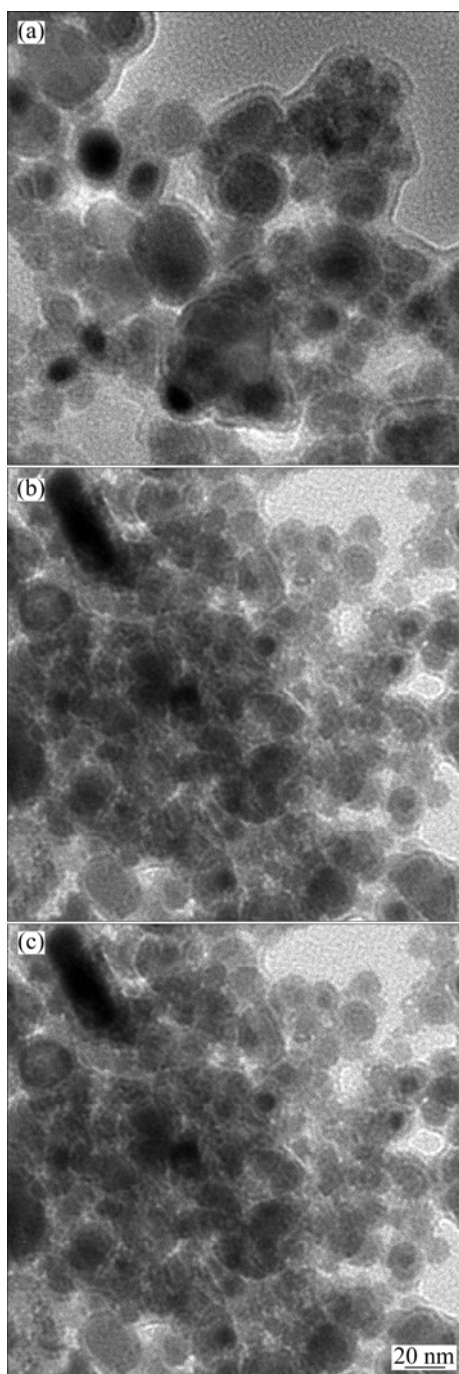


Fig. 2 TEM images of Sn nanoparticles sampled at varying rates of centrifugation for centrifugate/solvent exchange: (a) 6000 r/min; (b) 10000 r/min; (c) 12000 r/min

collisions between Sn nanoparticles in the bottom region of the glass tube. Although the Sn nanoparticles were solid and covered with a thin PVP capping and oxide layer, the agglomeration behavior observed among them was astonishing. Sn has a low melting point (232 °C) and hence can probably show high diffusivity at room temperature. For example, the grain-boundary diffusivity of Sn (D_{GB}) at 300 K has been reported as $1.45 \times 10^{-8} \text{ cm}^2/\text{s}$ [11]. According to Fick's 2nd law, diffusion distance (x) can be determined as $x = (Dt)^{1/2}$, where D is the diffusivity and t is the diffusion time. Therefore, Sn atoms can diffuse up to a distance of 1.2 μm along the grain-boundary in only 1 s. Consequently, the agglomeration that results in the formation of neck structures can probably be completed during contact between nanoparticles. This process is probably even when thin surface oxide layers act as barriers during the inter-diffusion between Sn nanoparticles. The thin PVP capping layer would burst owing to collisions between nanoparticles.

Figure 3 shows DSC results of pure DEG and DEG solution containing as-synthesized Sn nanoparticles. In case of pure DEG, a large endothermic peak was detected at about 183.7 °C, indicating the evaporation of DEG. On the other hand, the DSC results for DEG containing Sn nanoparticles showed an additional endothermic peak at 191.7 °C besides the evaporation peak. The presence of the additional peak was attributed to the melting of Sn nanoparticles. Decrease in the melting point of Sn with the decrease in the particle size on a nano-scale has been frequently reported theoretically and experimentally [3,10,12]. The melting point of Sn nanoparticles with a diameter of 13.1 nm coincides well with the endothermic peak at 191.7 °C.

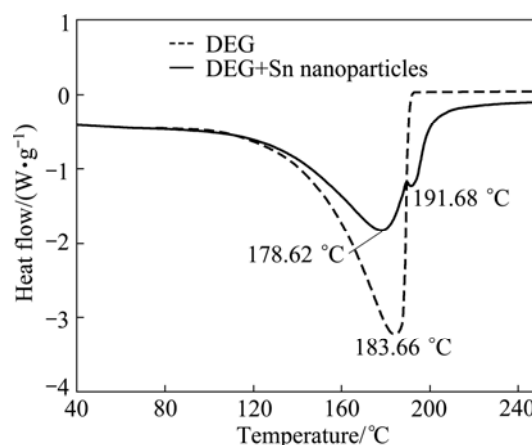


Fig. 3 DSC results of pure DEG and DEG containing Sn nanoparticles

Figure 4 shows the DSC results of methanol solution containing Sn nanoparticles after solvent exchange by centrifugation at 6000–12000 r/min. If

methanol evaporation peaks below 65 °C were exempted, slightly broad melting peaks were observed to be shifted to 224.8–225.8 °C, which indicated a change in the size or shape of Sn nanoparticles. According to previous reports on the relationship between the size and melting point of Sn nanoparticles, a melting point of 225 °C corresponds to a diameter of about 30 nm [10]. Therefore, it was hypothesized that the agglomerates observed in Figs. 2(a)–(c) influenced the peak shift of about 33.3 °C at higher temperatures. The agglomerated structure of nanoparticles may reduce the extent of decrease in the melting point of nanoparticles. The formation of new bonds between nanoparticles results in a decrease in the internal energy as nanoparticles find a more stable configuration by decreasing their unstable surface area. Hence, the melting point of agglomerates is higher than that of isolated nanoparticles. With an increase in the centrifugal rate, the peak melting temperature increased slightly from 224.8 °C to 225.8 °C. This indicated that the degree of agglomeration slightly intensified with the increase in the centrifugal rate. In summary, as the number of isolated nanoparticles affecting the drop in melting point was abruptly reduced on centrifuging, the centrifugation process was detrimental to maintaining the reduced melting point of Sn nanoparticles.

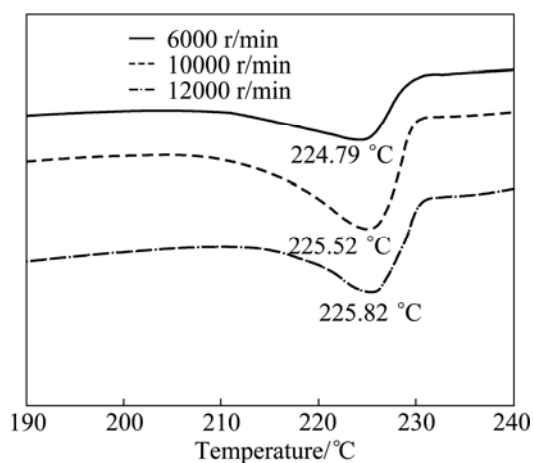


Fig. 4 DSC results of methanol solution containing Sn nanoparticles after solvent exchange by centrifuging at various centrifugation rates

Images of Sn nanoparticles that were dried after DEG was exchanged with methanol via repetitive centrifugation at various centrifugation rates are shown in Fig. 5. In this case, centrifugation was performed at a rate of 6000 r/min (Fig. 5(a)), and extensive aggregation was observed. The size and morphology of a unit lump of aggregated Sn nanoparticle were different from those observed in Fig. 2(a). The range and extent of aggregation was observed to be wider and more pronounced. Hence, it was concluded that the aggregation behavior of Sn nanoparticles continuously

intensified during the drying process after centrifugation. The sticky surface characteristics of Sn nanoparticles encapsulated with PVP may enhance aggregation of the nanoparticles during drying.

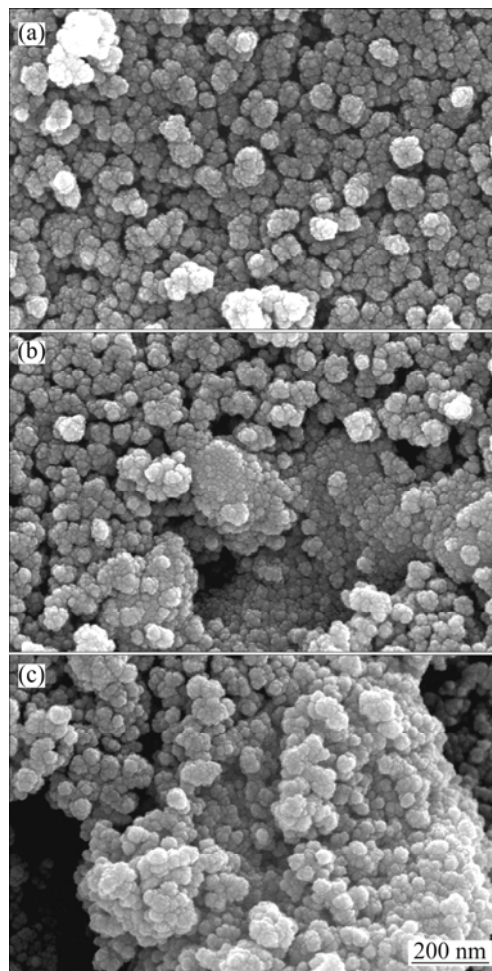


Fig. 5 FE-SEM images of dried Sn nanoparticles prepared as function of centrifugal rate: (a) 6000 r/min; (b) 10000 r/min; (c) 12000 r/min

Sn nanoparticles that were centrifuged at a rate of 10000 r/min (Fig. 5(b)) formed larger lumps because they underwent greater agglomeration during centrifugation. Similar to the case in Fig. 5(a), the aggregation behavior was observed to intensify with drying. Finally, Sn nanoparticles that were dried after centrifugation at a rate of 12000 r/min (Fig. 5(c)) formed very coarse lumps. As a result, the final size of the dried lumps increased with an increase in the rate of centrifugation. Further, the drying process intensified aggregation of the final particles, and a higher centrifugation rate increased the final size of the dried aggregates.

The effect of aggregation on the dried Sn nanoparticles can be further understood from the results of DSC, as shown in Fig. 6. The Sn aggregates that were

dried after centrifuging at a rate of 6000 r/min have a peak melting temperature of 223.9 °C. This indicated that aggregation during drying did not significantly result in the increase of the melting point. Further, the Sn aggregates that were centrifuged at rates of 10000 and 12000 r/min did not show a noticeable increase in the melting points after drying as compared to those of the nanoparticles in methanol solution. Consequently, the extensive aggregation behavior during drying did not influence the melting point of Sn nanoparticles. As mentioned above, aggregation during drying resulted from coalescence of PVP on the nanoparticle surface. Hence, the extensive aggregation behavior will not induce agglomeration of nanoparticles.

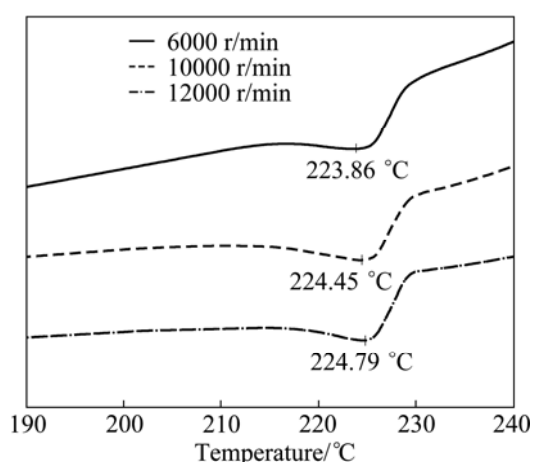


Fig. 6 DSC results of Sn aggregates dried after centrifugation at varying rates

4 Conclusions

Sn nanoparticles with an average diameter of 13.1 nm were synthesized by a modified polyol method. Because the melting temperature of the nanoparticles is 191.7 °C, a decrease of about 40 °C was observed for nanoparticles synthesized by this method. The relationship between the size and the melting temperature of a nanoparticle coincided well with previous reports. A centrifugation rate higher than 6000 r/min led to the formation of agglomerates with solid-state Sn nanoparticles. Hence, the number of isolated nanoparticles participating in the melting point drop was abruptly reduced in proportion with the centrifugal rate, resulting in an increase in the melting point. The drying process induced extensive aggregation in the final Sn nanoparticles mainly due to the stickiness

of the PVP capping material. However, the aggregation behavior did not additionally suppress the melting point drop because the agglomeration between nanoparticles observed after centrifuging did not occur in the aggregates.

References

- [1] KUMAR C. Metallic nanomaterials [M]. Weinheim: Wiley-VCH, 2009: 3.
- [2] ZOU C D, GAO Y L, YANG B, XIA X Z, ZHAI Q J, ANDERSSON C, LIU J. Nanoparticles of the lead-free solder alloy Sn–3.0Ag–0.5Cu with large melting temperature depression [J]. *Journal of Electronic Materials*, 2009, 38(2): 351–355.
- [3] JIANG H, MOON K, DONG H, HUA F, WONG C P. Size-dependant melting properties of tin nanoparticles [J]. *Chemical Physics Letters*, 2006, 429: 492–496.
- [4] HSIAO L Y, DUH J G. Revealing the nucleation and growth mechanism of a novel solder developed from Sn–3.5Ag–0.5Cu nanoparticles by a chemical reduction method [J]. *Journal of Electronic Materials*, 2006, 35(9): 1755–1760.
- [5] JIANG H, MOON K, HUA F, WONG C P. Synthesis and thermal and wetting properties of tin/silver alloy nanoparticles for low melting point lead-free solders [J]. *Chemistry of Materials*, 2007, 19: 4482–4485.
- [6] LIN C Y, MOHANTY U S, CHOU J H. Synthesis and characterization of Sn–3.5Ag–XZn alloy nanoparticles by the chemical reduction method [J]. *Journal of Alloys and Compounds*, 2009, 472: 281–285.
- [7] ZOU C, GAO Y, YANG B, ZHAI Q. Synthesis and DSC study on Sn3.5Ag alloy nanoparticles used for lower melting temperature solder [J]. *Journal of Materials Science: Materials in Electronics*, 2010, 21: 868–874.
- [8] LIN C Y, MOHANTY U S, CHOU J H. High temperature synthesis of Sn–3.5Ag–0.5Zn alloy nanoparticles by chemical reduction method [J]. *Journal of Alloys and Compounds*, 2010, 501: 204–210.
- [9] JO Y H, PARK J C, BANG J U, SONG H, LEE M H. New synthesis approach for low temperature bimetallic nanoparticles: Size and composition controlled Sn–Cu nanoparticles [J]. *Journal of Nanoscience and Nanotechnology*, 2011, 11: 1037–1041.
- [10] JO Y H, JUNG I, CHOI C S, KIM I, LEE H M. Synthesis and characterization of low temperature Sn nanoparticles for the fabrication of highly conductive ink [J]. *Nanotechnology*, 2011, 22: 225701–225708.
- [11] SELLERS M S, SCHULTZ A J, BASARAN C, KOFKE D A. β -Sn grain-boundary structure and self-diffusivity via molecular dynamics simulations [J]. *Physical Review B*, 2010, 81(13): 134111-1–134111-10.
- [12] LAI S L, GUO J Y, PETROVA V, RAMANATH G, ALLEN L H. Size-dependent melting properties of small tin particles: Nanocalorimetric measurements [J]. *Physical Review Letters*, 1996, 77(1): 99–102.

(Edited by YANG You-ping)